Available online at www.sciencedirect.com
ScienceDirect
Ceramics International 37 (2011) 2695–2700
CERAMICS INTERNATIONAL
www.elsevier.com/locate/ceramint

Synthesis of $Ba_2TiOSi_2O_7$ and $Ba_2TiOSi_{1.8}Ge_{0.2}O_7$ ferroelectric ceramics and the structure determination by Rietveld analysis

Shiv Kumar Barbar, M. Roy *

Department of Physics, M.L. Sukhadia University, Udaipur 313002, Rajasthan, India

Received 1 February 2011; received in revised form 9 April 2011; accepted 11 April 2011
Available online 15 April 2011

Abstract

Polycrystalline ceramic samples of pure fresnoite compound of formula $Ba_2TiOSi_2O_7$ and germanium (Ge^{4+}) doped compound $Ba_2TiOSi_{1.8}Ge_{0.2}O_7$ have been prepared by standard solid state reaction technique using high purity oxides and carbonates. The pure compound of fresnoite was sintered at 1300 °C while the Ge^{4+} substituted compound was sintered into pellet form at 1180 °C. The formation of the single phase compound was confirmed by X-ray diffraction (XRD) and the structural parameters were refined by the Rietveld analysis. A good agreement between observed and calculated X-ray diffraction pattern was obtained from the Rietveld refinement using noncentrosymmetric space group *P*4*bm*. The bond distances along with bond angles between atoms for both the compounds as well as the position of the atoms in the unit cell were calculated which supports the structural results. The grain size of both the compounds was investigated from SEM micrographs. The results are discussed in detail.
© 2011 Elsevier Ltd and Techna Group S.r.l. All rights reserved.

Keywords: A. Sintering; B. Grain size; B. X-ray method; D. Silicate; E. Structural applications

1. Introduction

A number of new barium bearing silicate minerals have been discovered during the course of geological study of the sanbornite deposits of eastern Fresno County, California. Fresnoite, a barium titanium silicate mineral of general formula $Ba_2TiOSi_2O_7$ is one of them [1]. It is a rare mineral and showing noncentrosymmetric tetragonal structure of point group 4*mm* with space group C_{4V}^2-*P*4*bm* [2]. Due to the noncentrosymmetric crystal structure, this material shows good ferro, piezo, pyro as well as optical and other nonlinear properties useful for different practical devices [3–10]. The electromechanical coupling factor of single crystal grown by Czochralski method is large enough ($k = 0.28$) for piezoelectric devices and hence it could be exploited as an alternate substrate material for surface acoustic wave (SAW) devices [11,12]. It is interesting to note that the single crystal data shows a broad peak in dielectric permittivity at ~433 K but the same peak is absent in dielectric loss curve. It is surprising that the ceramic samples fail to reveal a reproducible dielectric anomaly at 433 K shown in case of single crystal [4]. Not only that a small reproducible dielectric anomaly has also been reported in the frequency range 0.1–100 kHz at 805 K [13]. It was reported that an elastic anomaly observed at 435 K might likely be associated with a commensurate–incommensurate phase transition [14]. However, the single crystal X-ray data taken at 297 K and at 573 K revealed no change in symmetry except small change in atomic position, the largest of which were less than 0.02 Å [9]. It has also been reported that the differential scanning calorimetry (DSC) measurement from 300 to 875 K showed a wide (~60 K) reproducible thermal anomaly at 433 K with enthalpy change $\Delta H = 60(10)$ J mol^{-1} and corresponding entropy change $\Delta S = 0.19137$ J mol^{-1} K^{-1}. A thermal anomaly of comparable width was also observed at 810(5) K with $\Delta H = 160$ J mol^{-1} and $\Delta S = 0.2$ J mol^{-1} K^{-1} [13]. Uchida et al. suggested that the second order optical nonlinearity of the crystal was strongly affected by the distortion of the crystal structure [15]. Recent studies indicate that an optically transparent nanocrystallized glass demonstrate strong second harmonic generation (SHG) and blue photoluminescence, whereas the Sm^{3+} doped glass ceramic samples of fresnoite show visible up conversion luminescence by focused IR femtosecond laser pumping which

* Corresponding author. Tel.: +91 294 2423641; fax: +91 294 2423641.
E-mail address: mroy1959@yahoo.co.in (M. Roy).

0272-8842/$36.00 © 2011 Elsevier Ltd and Techna Group S.r.l. All rights reserved.
doi:10.1016/j.ceramint.2011.04.018

was enhanced by heat treatment [16,17]. Latest investigation indicates that the glassy fresnoite revealed anomalous boson behavior suggesting that an elastically softer region exists at the interface of the fresnoite nucleus/crystallite in the super cooled liquid state [18]. Recent studies on oriented crystallization using thermal gradient, crystallization kinetics and electrical properties through impedance spectroscopy were also carried out on fresnoite and fresnoite like glassy materials [19–22]. The ceramic sample also showed good hysteresis loop at room temperature but the shape of the loop remained unchanged when temperature increased to 875 K. It is surprising that the high temperature X-ray, DTA and specific heat measurements gave no indication of phase transition.

From the existing literature it has been observed that different authors have tried to investigate, analyze and understand the anomalous physical behavior using different experimental techniques but the adequate explanation is still lacking and need further improvements. Apart from the existing literature, no literature reports on structural refinement using Rietveld analysis and its other physical properties either in single crystal or in ceramic form except glass ceramics [23] to understand the electronic behavior in bulk. Because of the technological importance and interesting physical properties, it is necessary to understand the crystal structure of these materials. The present paper reports on the synthesis, detailed structural analysis using the Rietveld refinement method and morphological properties of pure and 10% Ge-doped fresnoite compounds.

2. Experimental

The polycrystalline ceramic samples of pure and Ge-substituted fresnoite compounds of chemical compositions $Ba_2TiOSi_2O_7$ and $Ba_2TiOSi_{1.8}Ge_{0.2}O_7$ were prepared by conventional solid state reaction technique using high purity carbonates and oxides [$BaCO_3$, TiO_2, GeO_2 and SiO_2 (99.9% pure obtained from CDH Bombay and E-MERCK Germany)]. Stoichiometric mixture of these oxides and carbonates was thoroughly mixed in liquid medium for several hours and then calcined at 800 °C for 8 h and at 900 °C for 8 h in silica crucible in air atmosphere. The process of mixing and calcination was repeated until a fine homogeneous powder of the material was obtained. The resulting mixture was compressed into pellet form by applying pressure around 5 tones/cm^2 (498 MPa) using hydraulic press. The pellets of pure sample ($X = 0.0$) were completely melted when heated to 1300 °C for 0.5 h in an electric furnace. The melted sample was cooled at the rate of 1 °C/min down to 1100 °C then further cooled at higher rate up to room temperature. The melted sample was scratched from the platinum crucible and repelletized after grinding. Now, these pellets were sintered at 1100 °C for 45 min and then electroded with silver paint for electrical measurement. The pellets of Ge-doped samples were sintered at 1180 °C for 2 h. The color of pellets was changed from white to light yellow after the sintering. The formation of the single phase compound was checked by X-ray diffraction pattern using the Rigaku X-ray diffractometer with CuKα radiation and nickel filter in a wide range of 2θ from 10° to 90° with a scanning rate of 2°/min. The instrument was calibrated using the pure silicon sample provided with the instrument. The lattice parameters and other crystal structural information such as bond distances, bond angles, atomic position in a unit cell etc. were obtained by the Rietveld refinement program 'Fullprof' using a Pseudo-Voigt function. The surface morphology and grain size of the samples were measured by scanning electron microscopy (SEM) using the JEOL, JSM-5600 SEM with different magnifications in back scattered mode.

3. Results and discussion

The room temperature (RT) X-ray diffraction patterns of the samples $Ba_2TiOSi_2O_7$ and $Ba_2TiOSi_{1.8}Ge_{0.2}O_7$ are shown in Fig. 1. From the X-ray diffraction patterns, it is observed that all the X-ray peaks of the pure compound except two very low intensity peaks at $2\theta = 26.37°$ and 31.49°, are well matching with the JCPDS Card No. # 84-0294. From the X-ray diffraction pattern it is also observed that there is a small shift in some of the peaks positions and intensities for the substituted compound with respect to the pure compound. In spite of minor difference in some of the peak positions and intensities as well as absence of peak at 31.49°, 2θ position in Ge-doped compound, both the compounds show almost similar XRD pattern.

In the present study, we have adopted the Rietveld refinement technique to investigate the crystal structure of both the compounds. The Rietveld refinement of the X-ray data generated from the machine for both the compounds were performed with the program Fullprof [24] using a Pseudo-Voigt function convoluted with an axial divergence symmetry function and are shown in Fig. 2(a and b). The Rietveld analysis of both the compounds confirms a tetragonal structure with space group *P4bm* and point group 4*mm*. There is a good agreement between observed and calculated profile, which is confirmed by observing the difference between observed and calculated profile on the same scale. In the case of pure compound ($Ba_2TiOSi_2O_7$), the difference pattern shows two

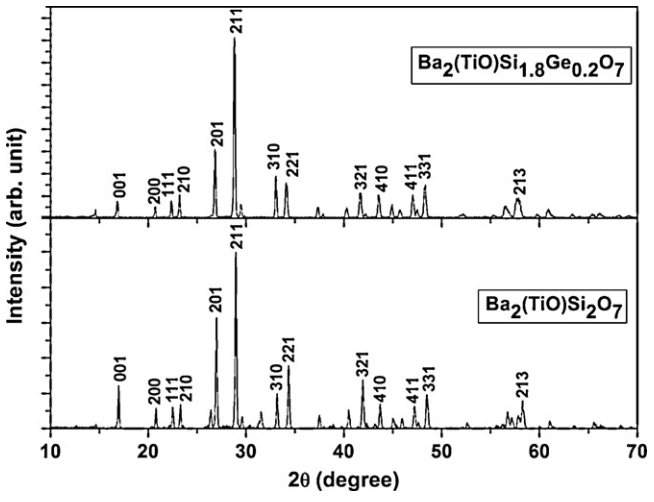

Fig. 1. RT X-ray diffraction patterns of $Ba_2TiOSi_2O_7$ and $Ba_2TiOSi_{1.8}Ge_{0.2}O_7$.

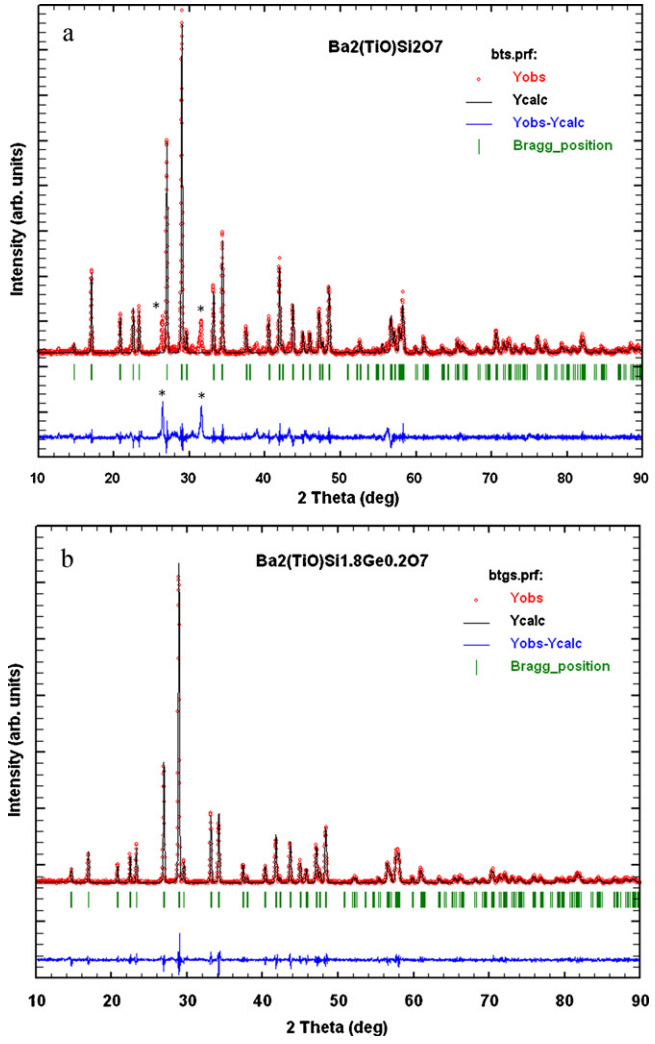

Fig. 2. (a) Rietveld refined profile of $Ba_2TiOSi_2O_7$. Observed (. . .), calculated (continuous line) and the difference between observed and calculated profile is plotted below on the same scale. (b) Rietveld refined profile of $Ba_2TiOSi_{1.8}Ge_{0.2}O_7$. Observed (. . .), calculated (continuous line) and the difference between observed and calculated profile is plotted below on the same scale.

low intensity peaks which are the impurity peaks and has not been fitted in the present case. This impurity phase peak at $2\theta = 26.37^\circ$ and 31.49° may be due to the formation of $BaTiO_3$ and TiO_2 which is within 5% of the total error and coming within the error limit. The detailed X-ray analysis of the pure compound was reported in our earlier paper [25]. Further analysis reveals that there is no impurity peak for substituted compound ($Ba_2TiOSi_{1.8}Ge_{0.2}O_7$) in Rietveld refined pattern. The detailed analysis results such as cell parameters, R_{Bragg}, etc. are summarized in Table 1. There is also a good agreement between observed (based on Bragg's condition i.e. $2d$ sin $\theta = n\lambda$) and calculated (based on refined cell parameters) d-values for both the compounds and are shown in Table 2. From the table it is observed that, there is a significant change in d-values for the substituted compound i.e. the lattice spacing (d-values) increases for the doped compound. This significant change in d-values due to the substitution of Ge^{4+} ion may be explained in terms of difference in ionic radii of Ge^{4+} with that of Si^{4+}. As the size of Ge^{4+} ion (0.53 Å) is larger in comparison with that of Si^{4+} (0.4 Å), the d-spacing of substituted compounds increases. But the tetragonality of both the compounds are almost constant having the value of 0.61 (Table 1) and hence the same crystal structure.

Table 1
Detailed Rietveld refined parameters for $Ba_2TiOSi_2O_7$ and $Ba_2TiOSi_{1.8}Ge_{0.2}O_7$.

Powder data		
Chemical formula	$Ba_2TiOSi_2O_7$	$Ba_2TiOSi_{1.8}Ge_{0.2}O_7$
Formula weight	506.70	515.61
Formula unit per cell	2	2
Space group	*P4bm*	*P4bm*
Crystal symmetry	Tetragonal	Tetragonal
Refinement		
Centrosymmetric	Acentric	Acentric
a (Å)	8.542	8.551
c (Å)	5.220	5.222
Tetragonality (c/a)	0.61	0.61
Unit cell volume (Å^3)	381.083	383.437
Bragg R-factor	2.66	2.39
R_f-factor	2.44	2.01
R_p	17.6	17.8
R_{wp}	24.6	24.8
R_{exp}	9.69	20.6
GOF (R_{wp}/R_{exp})	2.5	1.2
χ^2	6.447	1.423

The interatomic distances (bond distances/bond lengths) together with the bond angles were calculated by using the program *Bond_Str* and are shown in Tables 3 and 4. The position of atoms in the unit cells was calculated using the program Fullprof Studio. Calculations of errors in bond distances took into accounts the errors in the cell dimensions

Table 2
Comparison between some of the observed and calculated d-values for $Ba_2TiOSi_2O_7$ and $Ba_2TiOSi_{1.8}Ge_{0.2}O_7$ after Rietveld refinement.

$Ba_2TiOSi_2O_7$			$Ba_2TiOSi_{1.8}Ge_{0.2}O_7$			$h\,k\,l$
2θ	d-obs	d-cal	2θ	d-obs	d-cal	
16.973	5.222	5.220	16.888	5.248	5.245	0 0 1
20.780	4.273	4.271	20.759	4.277	4.275	2 0 0
22.494	3.951	3.949	22.420	3.964	3.962	1 1 1
23.265	3.822	3.82	23.241	3.825	3.824	2 1 0
26.951	3.307	3.306	26.880	3.315	3.314	2 0 1
28.940	3.084	3.083	28.869	3.091	3.090	2 1 1
29.553	3.021	3.020	29.523	3.024	3.023	2 2 0
33.136	2.702	2.701	33.102	2.705	2.704	3 1 0
34.275	2.615	2.614	34.205	2.620	2.619	2 2 1
37.510	2.397	2.396	37.342	2.407	2.406	1 1 2
40.472	2.228	2.227	40.309	2.236	2.235	2 0 2
41.838	2.158	2.157	41.765	2.161	2.161	3 2 1
43.653	2.073	2.072	43.607	2.074	2.073	4 1 0
44.986	2.014	2.013	44.939	2.016	2.015	3 3 0
45.874	1.977	1.977	45.798	1.980	1.979	4 0 1
47.158	1.926	1.926	47.081	1.929	1.928	4 1 1
48.416	1.879	1.879	48.338	1.882	1.881	3 3 1
52.095	1.755	1.754	51.939	1.759	1.759	3 2 2
56.641	1.624	1.624	56.556	1.626	1.625	4 3 1
57.789	1.595	1.594	57.632	1.598	1.598	3 3 2
58.219	1.584	1.583	57.947	1.590	1.590	2 1 3
60.999	1.518	1.518	60.908	1.520	1.519	5 2 1

Table 3
Bond distances and bond angles for $Ba_2TiOSi_2O_7$ compound.

Bond type	Bond angle (°)	Bond distances (Å)		
		d_{12}	d_{23}	d_{13}
O1–Ba–O2	157.503	2.87524	2.22832	5.00711
O1–Ba–O3	88.668	2.87524	3.01222	4.11556
O2–Ba–O3	71.206	2.22832	3.00682	3.11278
O3–Ba–O4	38.729	3.01222	2.13368	3.35037
O3–Ti–O4	79.296	1.94397	1.28994	2.12404
O1–Si–O2	80.654	1.58548	3.11006	3.25343
O1–Si–O3	110.038	1.58548	1.49013	2.52058
O2–Si–O3	76.246	3.11006	1.49013	3.11278
Ba–O3–Ti	103.986	3.01222	1.94397	3.96018
Ba–O1–Si	99.530	2.87524	1.58548	3.50576
Ba–O2–Si	117.589	2.22832	2.14391	3.73990
Ba–O3–Si	89.077	3.01222	1.49013	3.33908
Ti–O3–Si	158.033	1.94397	1.49013	3.37231

and in the atomic coordinates. The bond distances and bond angles are in good agreement with the earlier report [2], although the present values are more precise. The structural refinement results given by Moore and Louisnathan [2] and Markgraf et al. [9] are well matching with the present work. The single crystal data indicates that the interatomic distance Ba–O varies from 2.65 Å to 3.34 Å [9]. But, the current structure refinement on ceramic sample of fresnoite indicates that the Ba–O distances varies from 2.13 Å to 3.01 Å with an obtuse angle O1–Ba–O2 (157.5°) and acute angles such as O2–Ba–O3 (71.2°), O3–Ba–O4 (38.72°) and O1–Ba–O3 (88.68°). This small variation in distances may be due to the samples in single crystal and ceramic form. It is also observed that most of the Ba–O distances are between 2.22 Å and 2.90 Å that are significantly shorter than the ionic bond length of 2.94 Å, indicating the presence of covalent character in these Ba–O bonds [2]. In both the Ti–O bond distances, a longer bond Ti–O3 (1.94 Å) and a shorter bond Ti–O4 (1.29 Å), disagrees with the values reported by Moore and Louisnathan [2] but shows good agreement with the values reported by Markgraf et al. [9]. Table 3 also presents the inter atomic distances between Si and O such as two shorter bonds (Si–O1 and Si–O3), one longer bond (Si–O2) and the acute angles, where the values are nearly correspond to those found in a pyrosilicate group. It is investigated that for the pure compound there are 53 bonds among Ba–Ba, Ba–O, Ti–O, Si–Si, Si–O and O–O atoms whereas for the Ge-substituted compound there are 58 bonds. It is noticed that with the substitution of Ge^{4+} ion on Si^{4+} site, the bonds Si–O–Si are broken and contribute to the formation of new bonds between Ge–O–Si and Ge–O–Ge. The bond distances and bond angles of germanium doped compound are summarized in Table 4.

Table 4
Bond distances and bond angles for $Ba_2TiOSi_{1.8}Ge_{0.2}O_7$ compound.

Bond type	Bond angle (°)	Bond distances (Å)		
		d_{12}	d_{23}	d_{13}
O1–Ba–O2	116.061	2.65471	2.76750	4.60023
O1–Ba–O3	99.381	2.65471	3.04673	4.35510
O2–Ba–O3	75.086	2.76750	2.88593	3.44624
O3–Ba–O4	27.545	2.88593	2.93278	5.17033
O3–Ti–O4	127.766	2.51179	0.60996	2.92537
O1–Si–O2	57.740	1.78319	1.17113	1.52381
O1–Si–O3	123.183	1.78319	1.65718	3.02669
O2–Si–O3	127.564	1.17113	1.65718	2.54640
O1–Ge–O2	57.740	1.52381	1.78319	1.17113
O1–Ge–O3	123.183	1.78319	1.65718	3.02669
O2–Ge–O3	127.564	1.17113	1.65718	2.54640
O3–Ge–O4	54.857	2.92537	1.65718	3.54645
Ba–O3–Ti	120.973	2.88593	2.51179	4.70093
Ba–O1–Si	104.500	2.65471	1.78319	3.54934
Ba–O2–Si	119.410	2.82446	1.17113	3.54934
Ba–O3–Si	105.834	2.88593	1.65718	3.69929
Ba–O1–Ge	104.500	2.65471	1.78319	3.54934
Ba–O2–Ge	108.228	2.76750	1.17113	3.32539
Ba–O3–Ge	105.834	2.88593	1.65718	3.69929
Ti–O3–Si	107.032	2.51179	1.65718	3.39025
Ti–O3–Ge	107.032	2.51179	1.65718	3.39025
Ge–O1–Si	0.38866	0.01209	1.78319	1.78319
Ge–O2–Si	0.59149	0.01209	1.17113	1.17113
Ge–O3–Si	0.28046	0.01209	1.65718	1.64820

The unit cell diagram of pure fresnoite and its Ge-substituted compound were generated with the help of the program *Fullprof Studio* using the refined cell parameters, space group

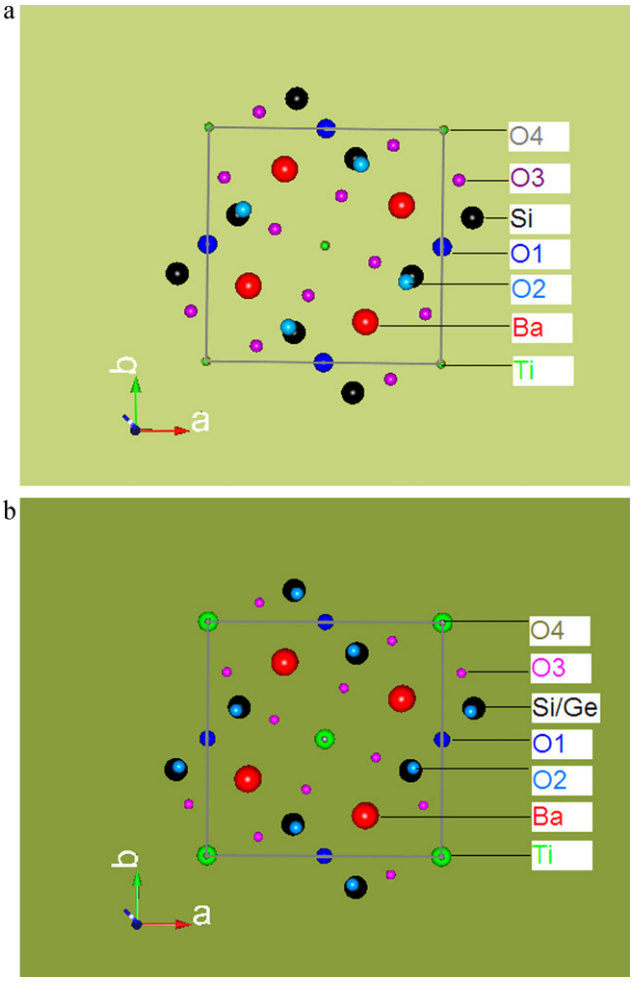

Fig. 3. (a) Unit cell diagram for $Ba_2TiOSi_2O_7$. (b) Unit cell diagram for $Ba_2TiOSi_{1.8}Ge_{0.2}O_7$.

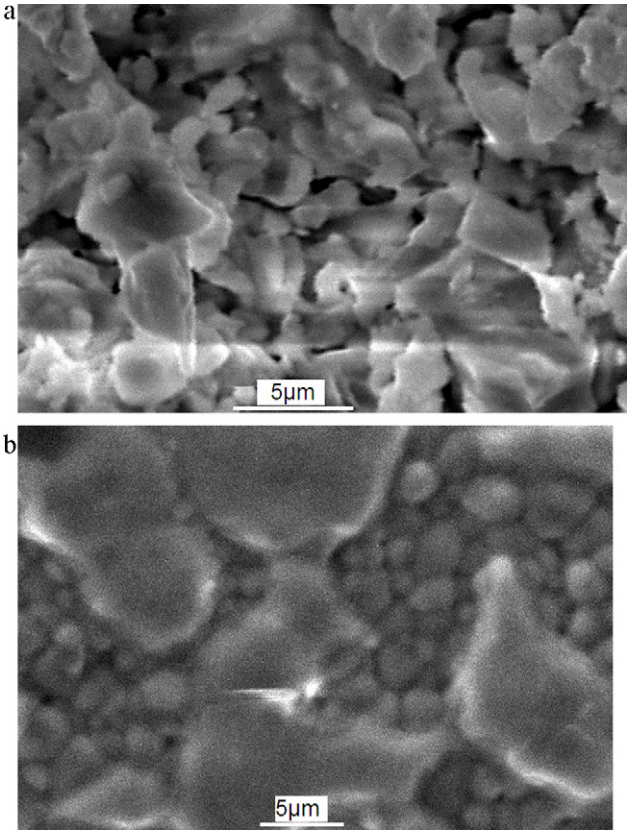

Fig. 4. (a) SEM micrograph of $Ba_2TiOSi_2O_7$. (b) SEM micrograph of $Ba_2TiOSi_{1.8}Ge_{0.2}O_7$.

and *xyz* coordinates of the atoms. Fig. 3a and b shows the unit cell diagrams of pure fresnoite and Ge^{4+}-doped compound. The unit cell of each compound contains 26 atoms. Hence, a unit cell for both the compounds of tetragonal crystal structure have two (2) formula units per unit cell. In case of pure compound the unit cell contains 4 atoms of barium (Ba), 2 atoms of titanium (Ti), 4 atoms of silicon (Si) and 16 atoms of oxygen (O1–2, O2–4, O3–4 and O4–2) whereas in case of Ge-doped compound the unit cell contains 4 atoms of Ba, 2 atoms of Ti, 4 atoms of Si + Ge and 16 atoms of oxygen (O1–2, O2–4, O3–2 and O4–8). This shows that both compounds have similar structure.

The morphological and microstructural properties of both the compounds were investigated using SEM. The typical SEM micrographs of both the samples are shown in Fig. 4(a and b). The micrographs show that the grain distributions are nearly uniform in pure compound and spherical throughout the surface except few in the Ge-doped compound. The grain size measured from these micrographs is around 2–3 μm for pure compound and around 2 μm for doped compound.

4. Conclusion

Analyzing the X-ray results it is concluded that a good agreement between the observed and calculated X-ray powder diffraction patterns was obtained by Rietveld refinement using noncentrosymmetric space group *P4bm* confirming the tetragonal structure. The overall crystal structure remains the same for both the compounds. Calculated bond distances and bond angles are in good agreement with the earlier report. Using the refined data the unit cell of the compound has been generated which contains two formula unit. The uniform microstructures of the compounds are responsible for good dielectric and ferroelectric behavior useful for different functional devices which will be discussed elsewhere.

Acknowledgement

Financial support from the University Grant Commission Project No: 36-178/2008 (SR) and UGC Fellowship to one of the authors (S.K. Barbar) is gratefully acknowledged.

References

[1] J.T. Alfors, M.C. Stinson, R.A. Matthews, A. Pabst, Seven new barium minerals from eastern Fresno County, California, Am. Mineral. 50 (1965) 314–340.
[2] P.B. Moore, S.J. Louisnathan, The crystal structure of fresnoite, $Ba_2(TiO)Si_2O_7$, Zeitschrift fur Kristallographie. Bd. 130 (1969) 438–448.
[3] S.C. Abrahams, Structurally based prediction of ferroelectricity in inorganic materials with point group 6 mm, Acta Crystallogr. B 44 (1988) 585–595.
[4] A. Halliyal, A.S. Bhalla, S.A. Markgraf, L.E. Cross, R.E. Newnham, Unusual pyroelectric and piezoelectric properties of fresnoite ($Ba_2TiSi_2O_8$) single crystal and polar glass-ceramics, Ferroelectrics 62 (1985) 27–38.
[5] M. Kimura, Y. Fujino, T. Kawamura, New piezoelectric crystal: synthetic fresnoite ($Ba_2TiSi_2O_8$), Appl. Phys. Lett. 29 (1976) 227–228.
[6] M. Kimura, Elastic and piezoelectric properties of $Ba_2TiSi_2O_8$, J. Appl. Phys. 48 (1977) 2850–2856.
[7] S. Haussühl, J. Eckstein, K. Recker, F. Wallrafen, Growth and physical properties of fresnoite $Ba_2TiSi_2O_8$, J. Cryst. Growth 40 (1977) 200–204.
[8] P.S. Bechthold, S. Haüssuhl, E. Michael, J. Eckstein, K. Recker, F. Wallrafen, Second harmonic generation in fresnoite, $Ba_2TiSi_2O_8$, Phys. Lett. A 65 (1978) 453–454.
[9] S.A. Markgraf, A. Halliyal, A.S. Bhalla, R.E. Newnham, C.T. Prewitt, X-ray structure refinement and pyroelectric investigation of fresnoite, $Ba_2TiSi_2O_8$, Ferroelectrics 62 (1985) 17–26.
[10] Y. Takahashi, K. Kitamura, Y. Benino, T. Fujiwara, T. Komatsu, Second-order optical nonlinear and luminescent properties of $Ba_2TiSi_2O_8$ nanocrystallized glass, Appl. Phys. Lett. 86 (2005) 091110–91111.
[11] H. Yamauchi, Surface-acoustic-wave characteristics on fresnoite ($Ba_2TiSi_2O_8$) single crystal, J. Appl. Phys. 49 (1978) 6162–6164.
[12] J. Melngailis, J.F. Vetelno, A. Jhunjunwala, T.B. Reed, R.E. Fahey, E. Stein, Surface acoustic wave properties of fresnoite, $Ba_2Si_2TiO_8$, Appl. Phys. Lett. 32 (1978) 203–205.
[13] M.C. Foster, D.J. Arbogast, R.M. Nielson, P. Photinos, S.C. Abrahams, Fresnoite: a new ferroelectric mineral, J. Appl. Phys. 85 (1999) 2299–2303.
[14] Z.P. Chang, A.S. Bhalla, Elastic anomaly in fresnoite ($Ba_2TiSi_2O_8$) single crystal, Mater. Lett. 8 (1989) 418–420.
[15] N. Uchida, S. Tanaka, K. Uematsu, T. Fujiwara, T. Komatsu, Molecular orbital approach to the optical nonlinearities of fresnoite-type crystals, J. Eur. Ceram. Soc. 27 (2007) 531–533.
[16] Y. Takahashi, K. Kitamura, S. Inoue, Y. Benino, T. Fujiwara, T. Komatsu, Effect of heat-treatment temperature on optical properties of $Ba_2TiSi_2O_8$ nanocrystallized glasses, J. Ceram. Soc. Jpn. 113 (2005) 419–423.
[17] B. Zhu, S. Zhang, G. Lin, S. Zhou, J. Qiu, Enhanced multiphoton absorption induced luminescence in transparent Sm^{3+}-doped $Ba_2TiSi_2O_8$ glass-ceramics, J. Phys. Chem. C 111 (2007) 17118–17121.

[18] Y. Takahashi, M. Osada, H. Masai, T. Fujiwara, Softer region at boundary of supercooled liquid–crystal in glassy fresnoite, Appl. Phys. Lett. 94 (2009) 241909–241911.
[19] Y. Ochi, T. Meguro, K. Kakegawa, Orientated crystallization of fresnoite glass-ceramics by using a thermal gradient, J. Eur. Ceram. Soc. 26 (2006) 627–630.
[20] B. Rangarajan, T. Shrout, M. Lanagan, Crystallization kinetics and dielectric properties of fresnoite $BaO–TiO_2–SiO_2$ glass ceramics, J. Am. Ceram. Soc. 92 (2009) 2642–2647.
[21] T. Park, M.J. Davis, P. Vullo, T.M. Nenoff, J.L. Krumhansl, A. Navrotsky, Thermochemistry and aqueous durability of ternary glass forming Ba-titanosilicates: fresnoite ($Ba_2TiSi_2O_8$) and Ba–titanite ($BaTiSiO_5$), J. Am. Ceram. Soc. 92 (2009) 2053–2058.
[22] B. Rangarajan, S.S.N. Bharadwaja, E. Furman, T. Shrout, M. Lanagan, Impedance spectroscopy studies of fresnoite in $BaO–TiO_2–SiO_2$ system, J. Am. Ceram. Soc. 93 (2010) 522–530.
[23] Y. Ochi, Fresnoite crystal structure in glass-ceramics, Mater. Res. Bull. 41 (2006) 740–750.
[24] J. Rodriguez-Carvajal, Recent developments of the Program FULL-PROF, in commission on powder diffraction, IUCr Newslett. 26 (2001) 12–19.
[25] M. Roy, S.K. Barbar, P. Dave, S. Jangid, InduBala, X-ray, scanning electron microscopy and electrical properties of synthetic fresnoite ($Ba_2TiSi_2O_8$) ceramics, Appl. Phys. A 100 (2010) 1191–1196.